Structure Development in Oriented Polyethylene Films and Microporous Membranes as Monitored by Sound Propagation

M. RAAB,[1] J. ŠČUDLA,[1] A. G. KOZLOV,[2] V. K. LAVRENTYEV,[2] G. K. ELYASHEVICH[2]

[1] Institute of Macromolecular Chemistry, Academy of Sciences of the Czech Republic, Heyrovsky Sq. 2., 162 06 Prague 6, Czech Republic

[2] Institute of Macromolecular Compounds, Russian Academy of Sciences, Bolshoi prospekt 31, 199004 St. Petersburg, Russia

Received 1 June 1999; accepted 7 June 2000

ABSTRACT: Microporous membranes of high-density polyethylene were prepared by melt-extrusion followed by annealing and uniaxial extension. Crystallization at a high melt flow rate and subsequent annealing of the spun films with fixed ends led to the formation of oriented hard-elastic materials with a high modulus of elasticity and a considerable work recovery. Uniaxial stretching of such systems along the orientation direction induced the formation of microscopic pores due to the specific structure of the hard-elastic material. At some critical values of the processing parameters, through-flow channels were formed, converting the film into a microporous membrane permeable to liquids and vapors. Sound propagation, tensile measurements, and X-ray diffraction techniques were used to characterize the structure and properties of the samples at individual stages of the process as a function of the processing parameters. In particular, it was shown that polar diagrams of the sound propagation velocity reflect sensitively the structural changes in the process of porous structure formation. © 2001 John Wiley & Sons, Inc. J Appl Polym Sci 80: 214–222, 2001

Key words: high-density polyethylene; polymer morphology; hard-elastic behavior; microporous membranes; sound propagation; X-ray diffraction

INTRODUCTION

Structural transformations of semicrystalline polymers represent an important way of controlling end-use properties. Under specific conditions, common-grade polymers can be converted to valuable polymer specialities. The properties of these products reflect their supermolecular structure. The supermolecular structure, in turn, is determined by crystallization conditions. Hard-elastic materials represent a typical example. These systems show not only a relatively high modulus of elasticity but—more importantly—also high elastic recovery similar to elastomers.[1,2]

The remarkable properties of hard-elastic systems are a direct consequence of their specific lamellar supermolecular organization. A necessary precondition for the formation of the hard-elastic structure is high-speed melt extrusion. It

Correspondence to: G. K. Elyashevich.

Contract grant sponsor: Russian Foundation of Fundamental Investigations; contract grant number: 98-03-33384a.

Contract grant sponsor: Grant Agency of the Academy of Sciences of the Czech Republic; contract grant number: A4050904.

Contract grant sponsor: Grant Agency of the Czech Republic; contract grant number: 106/98/0718.

Journal of Applied Polymer Science, Vol. 80, 214–222 (2001)

is suggested that upon annealing of such extruded material an array of large parallel lamellar crystals is formed with lamellar surfaces aligned perpendicularly to the orientation direction.[3] The deformation of these hard-elastic structures is *microscopically* heterogeneous: Under external stress, individual lamellae connected by distant bridges of tie chains bend and depart locally and, as a result, discontinuities (pores) appear in interlamellar spaces between the tie points.

The deformation mechanism of hard-elastic polymers differs from the cold drawing of common semicrystalline polymeric materials that is heterogeneous *macroscopically*, that is, plastic deformation is concentrated in a propagating neck shoulder. In a narrow zone of the active neck shoulder, there is a transformation of a lamellar (or spherullitic) structure into a fibrillar structure and, as a result, the strengthening of the initial material occurs.[4–6] On the other hand, no neck develops during the deformation of the hard elastics under typical conditions, but voids between individual deformed lamellae appear instead. The elasticity of hard-elastic polymers is of an energetic nature as its structural mechanism consists of lamellar bending. This is in contrast to the entropic deformation mechanism of typical rubbers or common semicrystalline polymers.

The formation of pores during the deformation of hard elastics is distinctly manifested only in a certain interval of strain rates. Other processes may prevail outside this experimental window: fracture at extremely high strain rates and some tendency to necking at very low strain rates. However, even within the conditions of pore formation, their number distinctly depends on the strain rate.[7]

Under certain processing conditions, the individual pores become interconnected, thus forming through-flow channels. Consequently, the film is transformed into a membrane permeable to liquids and gases.[7,8] The detailed conditions for obtaining the percolation threshold and the occurrence of through-flow channels connecting opposite membrane surfaces[7] are not completely understood. However, there is no doubt that the orientation, both on the molecular and supermolecular scales, together with the parameters of the crystalline structure (lamellar thickness, number of tie chains, distribution of tie chain length) play an important role here. The assessment of interrelations among the processing conditions, the structural parameters of the hard-elastic material, and the structure of the resulting membrane is the subject of the present study.

EXPERIMENTAL

Materials

Linear high-density polyethylene (Plastpolymer, Science-Industrial Co., St. Petersburg, Russia) with M_w = 140,000 and M_w/M_n = 6–8 and a melting temperature of 132°C was used as the starting material throughout this study. From this polymer, flat films were spun (laboratory extruder, SCAMIA, France) at 200°C with three different spin draw ratios λ: 14.5, 19.4, and 29.6. These extruded samples were annealed for 30 min at 130°C in a fixing frame to form hard-elastic films that were then extended to 200% to obtain microporous membranes.

Thus, nine different samples were the subject of the investigation. The samples were initially characterized by densities of 932 kg/m^3 for as-spun (extruded) films, 958 kg/m^3 for hard-elastic (annealed) films, and 600–630 kg/m^3 for porous membranes. The density values did not depend on the spin draw ratio.

X-ray Diffraction

Small-angle X-ray scattering (SAXS) was performed using a Kratky camera using CuKα radiation filtered by a Ni filter. The wide-angle X-ray scattering (WAXS) curves were obtained by a DRON-2.0 diffractometer with CuKα radiation.

The values of a long period for extruded and also for annealed samples were estimated from the SAXS curves. The orientation of the crystallites was characterized by an angle ψ (Fig. 1) between the orientation direction and the normal to the plane of the lamellae. The analysis of the SAXS data for these samples reveals two important characteristics: *First*, the lamellae are not perfectly perpendicular to the orientation direction but aligned in an angle (90 − ϕ) to the direction of orientation. Obviously, this angle characterizes the perfection of orientation. *Second*, there is scatter in the lamellar alignment. This is characterized by a disorientation angle α.

WAXS was used to obtain the degree of crystallinity and width of lamellae for as-spun and hard-elastic samples. The samples for transmission WAXS measurements were prepared by stacking several films together to a resulting

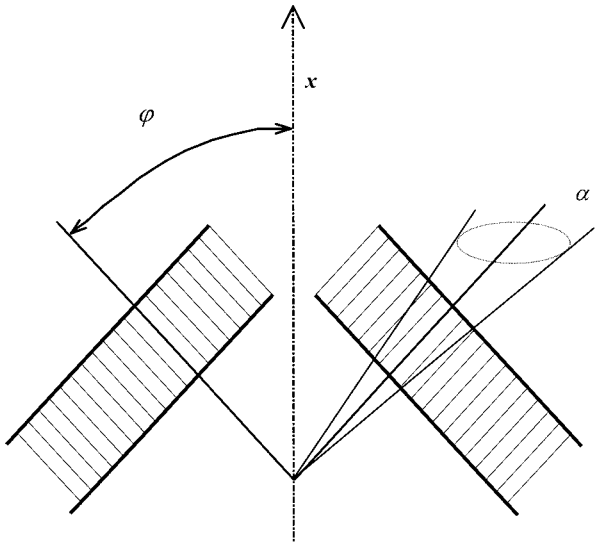

Figure 1 Definition of the angle φ characterizing the tilt of the lamellae against the orientation direction x and the angle of disorientation α.

thickness of about 1 mm. Integral intensities diffracted by the crystalline and amorphous phases were each used for the crystallinity determination.

Unfortunately, intensive diffuse scattering prevented an analysis of discrete reflections and the assessment of the long period in the case of SAXS for the microporous membranes. The intensity of this diffuse scattering reflecting microporosity increased with increasing sample orientation.[9]

Sound Propagation

Sonic velocity measurements were performed with a Pulse Propagation Meter PPM-R5 (manufactured by H. M. Morgan, Inc., USA). The apparatus produces sound pulses at a frequency of 5 kHz 197 times per second and measures electronically the time for the longitudinal sonic wave to pass through the film between transmit and receive transducers; the sonic velocity is then simply given by the ratio of the distance between the transducers and the transit time of a pulse.[10] The angular dependencies of the sonic velocity and the corresponding dependencies of the sonic modulus were determined for all samples under study.

Tested samples were fixed on their shorter sides in a frame without any stress. The position of one of the transducers was gradually varied along a chosen straight line (Fig. 2). The sonic velocity was determined by linear regression. The film was then rotated in its plane and the angle Φ between the given line and drawing direction varied from 0° (drawing direction) to 90° (cross direction) in 10° increments. Measurements were repeated at least five times along each line. From the average sound velocity v and its scatter, the sound modulus E_s and the corresponding standard deviation s_s were calculated as follows:

$$E_s = \rho_0\left(v^2 + \frac{k-1}{k}\, s_v^2\right) \tag{1}$$

$$s_s^2 = 4\rho_0^2 v^2 s_v^2 \tag{2}$$

where ρ_0 is the density of the material; k, the number of measurements; and s_v, the standard deviation of the sonic velocity v. The data of the sound velocity and of the sound modulus are then presented as polar diagrams.

Tensile Tests

Stress–strain tests were performed at a room temperature of 23°C and relative humidity of 45% using a tensile tester TIRATEST 2300 (manufactured by TIRA, Maschienenbau GmbH, Rauenstein, Germany). The test rate was always 250 mm/min. Test specimens were strips of 15 × 80-mm^2 with a gauge length of 60 mm. The specimens were cut from the films and membranes at various angles to the orientation direction varying between 0° and 90° with 10° increments.

RESULTS AND DISCUSSION

The structural and mechanical characteristics were studied for three stages of the sample preparation, namely, for as-spun (extruded) films,

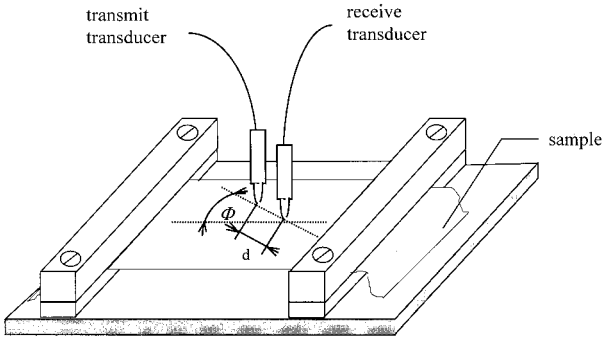

Figure 2 Adaptation of PPM apparatus for the measurement of sonic velocity in a planar film.

Table I Parameters of Crystalline Structure for Three Stages of Structure Formation

Structure Parameters	As-spun Films	Annealed Films	Membranes
Degree of crystallinity (%)	55	72	57
Long period (Å)	200	350	—
Lateral size of lamellae (Å)	200	300	180

hard-elastic (annealed) samples, and microporous membranes. All these samples were anisotropic, showing orientation of the crystallites (see also ref. 9).

As-spun Films

The structural parameters of initial as-spun films were characterized by SAXS and WAXS measurements. As shown by Table I, the parameters of the crystalline structure did not depend on the spin draw ratio λ. These values remained also unchanged at variations of flow velocity in the film-formation process. This result was not unexpected: It is well known[11,12] that these parameters are determined by crystallization and annealing temperatures but not by the dynamic conditions of film formation. In our experiments, as already reported earlier,[3,8,13] these temperatures were kept constant for all samples prepared within this study.

On the other hand, the angle $(90 - \varphi)$ reflecting the degree of orientation of extruded samples (see Fig. 1) increases with an increasing spin draw ratio λ. This is shown in Table II. At the same time, it appears that the angle of disorientation α does not depend on the spin draw ratio λ during the melt flow. These results may be explained by the fact that the angle φ as a parameter of orientation is controlled by the mechanical stress field developed in the melt during the extrusion and, consequently, depends on λ, while the angle α characterizing disorientation is affected by the melt temperature, which remained unchanged in our experiment. Obviously, the numerical value of φ depends on the extrusion temperature.

As indicated by the intensity of the X-ray scattering, the density of the amorphous phase and, consequently, also the number of tie molecules decrease with an increasing spin draw ratio: The scattering intensity for the sample with $\lambda = 19.4$ was twice lower than that for the sample formed at $\lambda = 14.5$. A decrease in the number of tie chains in the amorphous phase led to an increase of the distance between the tie points on the lamellar surfaces and, consequently, to an increase of the number and size of the pores. Consequently, the probability of through-flow channel formation also increased. Indeed, an increase of permeability of our membranes with increasing λ was already reported.[7]

Polar diagrams of the sound propagation velocity v for three as-spun films are presented in Figure 3. It can be seen that v decreases with an increasing spin draw ratio λ, particularly for its highest value ($\lambda = 29.6$). At the same time, the anisotropy of the sound velocity is most distinctly pronounced for the highest λ. The corresponding polar diagram shows maxima for directions declined by 50° to the orientation direction, in agreement with the X-ray results (see Table II). The observed decrease in sound velocity with increasing orientation obviously reflects lower structural continuity, for example, a lower number of tie chains as a consequence of intensive chain slipping at high velocities of the melt flow.

Table II Orientational Characteristics of Extruded Samples Differing in Spin Draw Ratio λ

λ	$(90 - \varphi)$ (°)	α (°)
14.5	43.5	11
19.4	47.2	10
29.6	53.6	11

Hard-elastic Films

As shown by the X-ray results, the annealing of the original extruded samples caused a substantial increase in lamellar thickness (see Table I). This can be ascribed to the incorporation of tie chains into the crystallites.[3,14] Thickening of crystalline lamellae is also reflected in the sound propagation but in a more complex way. In par-

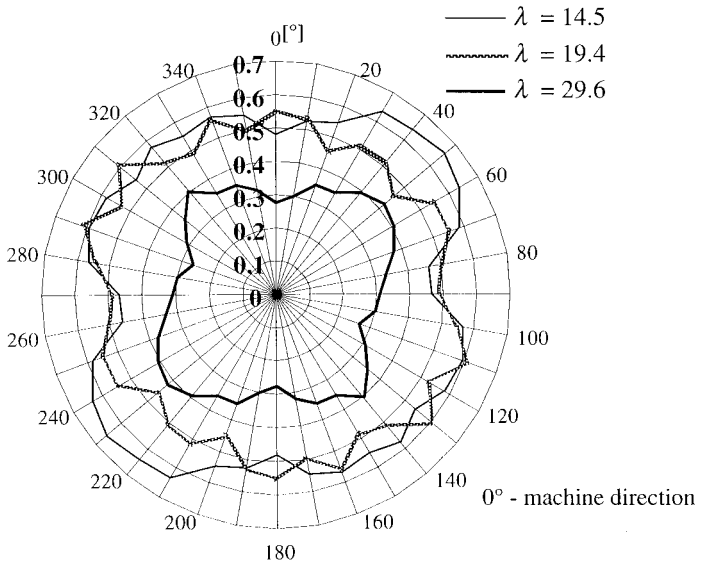

Figure 3 Polar diagrams of sound propagation velocity v (km s^{-1}) for three initial extruded films differing in spin draw ratio λ (indicated on the curves).

ticular, an interesting ("butterfly-type") pattern of the polar diagram was found for the annealed sample with the lowest original orientation (λ = 14.5). A relatively low initial orientation in this case was reflected in a marked bias in the orientation of crystallites (see Fig. 4), which is also preserved after annealing. The thickening of crystalline regions then results in a specific continuous crystalline structure. This is suggested by the polar diagram of sound velocity with four distinct maxima aligned 50° to the orientation direction (Fig. 4).

Certain anisotropy in sound propagation is also preserved for annealed samples with higher initial spin draw ratios (λ = 19.4 and 29.6). However, in this case, the absolute values of the sound velocity are markedly lower. This may be ascribed to a lower number of contacts between individual lamellae, that is, lower continuity of the crystalline phase. Nevertheless, all three annealed sam-

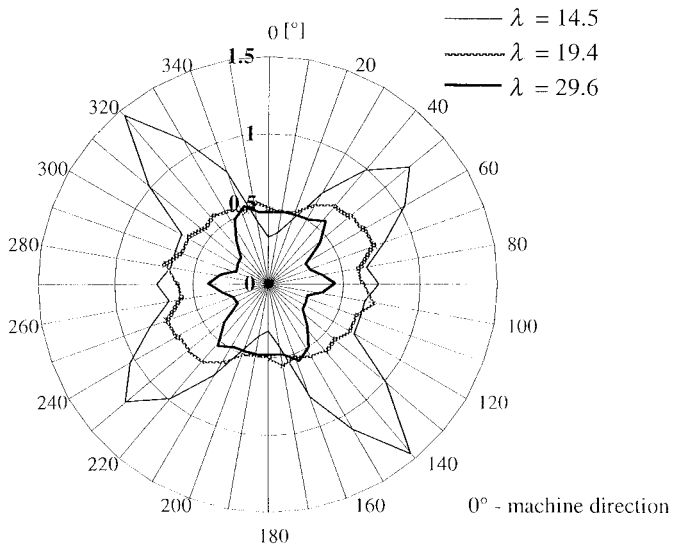

Figure 4 Polar diagrams of sound propagation velocity v (km s^{-1}) for three annealed films differing in the spin draw ratio λ of the initial films (indicated on the curves).

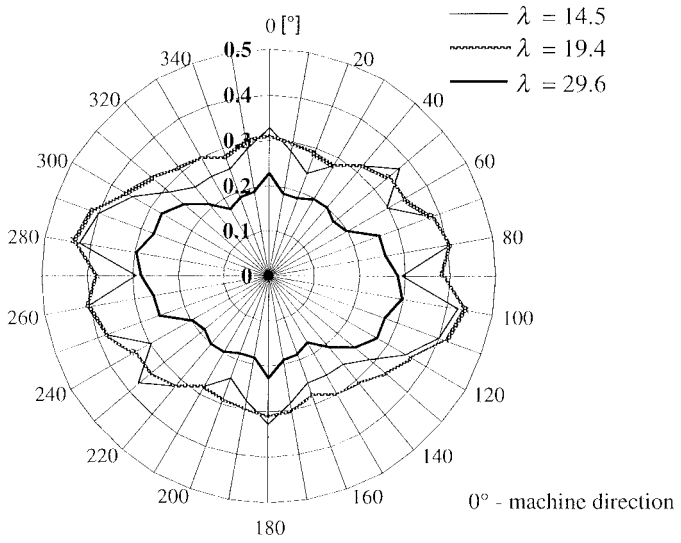

Figure 5 Polar diagrams of sound propagation velocity v (km s^{-1}) for three membranes differing in spin draw ratio λ of the initial films (indicated on the curves).

ples show virtually the same values of the sound velocity along the orientation direction.

Microporous Membranes

As already mentioned, intensive diffuse scattering prevents a detailed evaluation of the crystalline structure of microporous membranes by the SAXS method. The evaluation of the sound propagation offers here an alternative method. First, the velocity of the sound propagation in the porous membranes is substantially lower than is the velocity in hard-elastic films, particularly in the direction of orientation, at any value of λ. Another distinctive difference of the sound propagation in membranes as compared with extruded and annealed samples is the strong anisotropy of the sound velocity with maxima located perpendicularly to the orientation direction (Fig. 5). The "butterfly" pattern occurs again, but is less pronounced than for the hard-elastic films.

It should be noted that similar "butterfly-type" patterns were observed earlier by small-angle scattering of polarized light for microporous membranes immersed in a liquid that induced transparency.[9] The patterns were similar for various initial values of λ. On the other hand, no characteristic light-scattering patterns were observed for extruded and annealed films that were transparent for visible light.[15]

Elastic Modulus

Polar diagrams of the moduli for extruded, annealed, and porous samples with the original spin draw ratio λ of 19.4 are presented in Figure 6. Four pronounced maxima located at 0°, 90°, 180°, and 270° are expressed similarly to the extruded and annealed samples, reaching virtually the same values. Splitting of the maximum located along the draw direction for the annealed samples may reflect two prevailing angles of crystallite orientation. Similar splitting of maxima, both along and across the orientation directions, occurs also for porous membranes. For all three samples, the elastic modulus along the orientation direction is slightly higher than in the cross

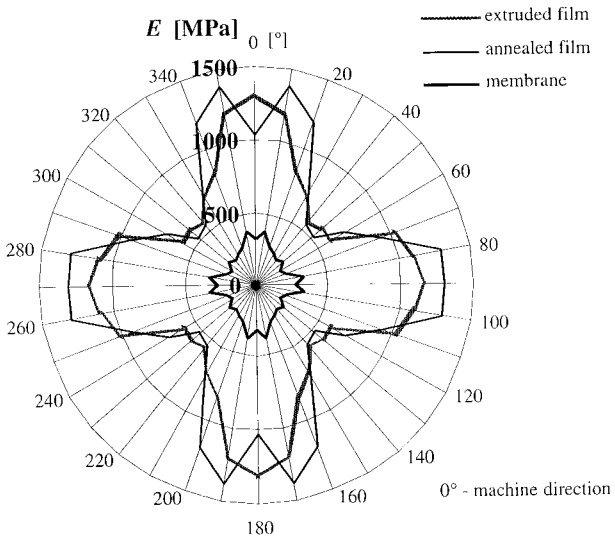

Figure 6 Polar diagrams of Young's modulus E for three stages of microporous membrane formation. The spin draw ratio λ of the initial film was 19.4.

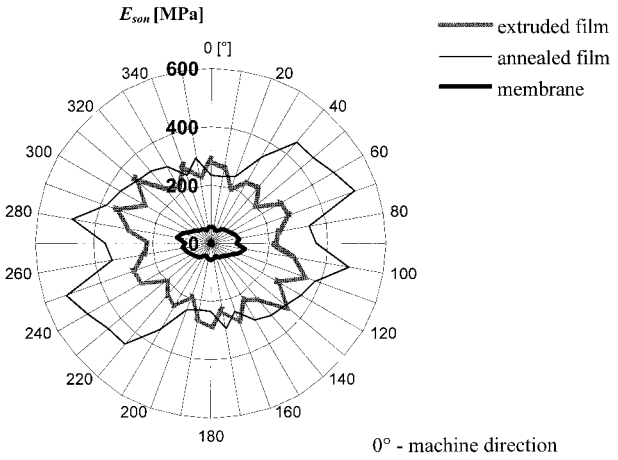

Figure 7 Polar diagrams of sonic modulus E_{son} calculated from the sonic velocity for three stages of microporous membrane formation. The spin draw ratio λ of the initial film was 19.4.

direction. However, absolute values of the Young's modulus for membranes decreased about three times as compared to the hard-elastic film. Obviously, this reflects the occurrence of heterogeneities.

Figure 7 shows polar diagrams of sound modulus values calculated from the sound velocities for the same three samples. It can be seen that sound moduli for all three samples are higher across the orientation direction than along the orientation. Broad maxima on the diagrams for the annealed samples are located between 40° and 70° and symmetrically between 220° and 250°.

Surprisingly, the values of the calculated sound modulus are distinctly lower for all samples as compared to the Young's modulus. The difference between the tensile and sound moduli is similar for the extruded and annealed samples, but is much more pronounced for the membranes. Besides, the polar diagrams of the tensile and sonic moduli differ in their shapes.

Structural Models

Structural models shown in Figures 8 and 9 can interpret the experimental results of the sound propagation obtained for the three stages of the porous structure formation. It is suggested that the original film oriented during melt extrusion contains crystalline lamellae interconnected by tie chains. In an ideal case of a very high spin draw ratio λ, these lamellae should be aligned perpendicularly to the orientation direction. At lower λ, the lamellae are somewhat declined, the declination increasing with decreasing λ. This situation is schematically shown in Figures 8(a) and 9(a). Upon annealing, the lamellar thickness increases. While in an ideal case the perfectly parallel lamellae still remain fully separated by an amorphous matrix, in a system of declined lamellae, the probability of their mutual contacts increases from a purely geometrical reason [Figs. 8(b) and 9(b)]. It is well known that sound velocity is higher in the crystalline phase than in an amorphous matrix. The "butterfly-type" of polar diagrams of the sound velocity with distinct maxima at particular angles could then be ascribed to continuous paths of the crystalline phase in certain directions. Figure 4 shows clearly that such a situation occurs only at low λ. At an intermediate λ, a maximum sound velocity is observed perpendicularly to the orientation direction, and in the case of the highest λ, the direction of the highest sound velocity coincides with the orientation direction.[16]

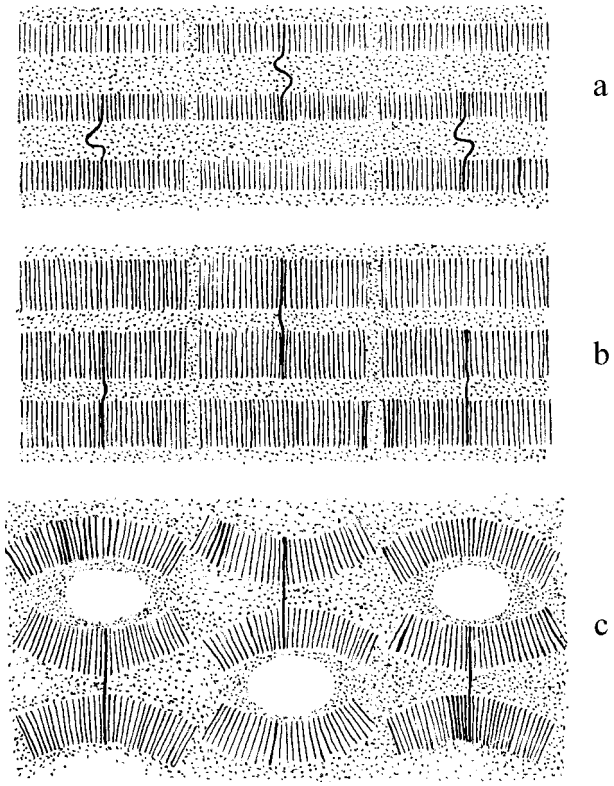

Figure 8 Schematic model of structure transformations from (a) an initial (extruded) film to (b) an annealed film and (c) a membrane for a high value of the spin draw ratio λ.

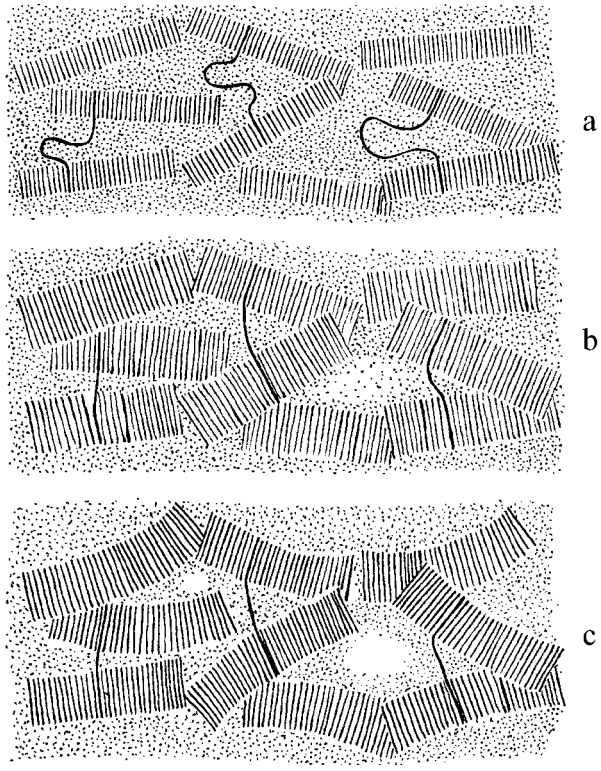

Figure 9 Schematic model of structure transformations from (a) the initial (extruded) film to (b) an annealed film and (c) a membrane for a low value of the spin draw ratio λ.

The formation of interlamellar pores in the third stage of the structure formation dramatically decreases the integrity of the crystalline structure, particularly in the orientation direction. This is directly illustrated by an SEM micrograph of the membrane surface (Fig. 10). Obviously, open pores represent the most effective obstacles to sound propagation. As a result, the absolute values of the velocity of sound propagation decrease in all directions, but particularly along the orientation. As shown in the schematic model, the best conditions for sound propagation in the porous structure now appear along the lamellae, that is, across the molecular chain direction. This is why the maximum value of sound propagation in the membranes now appears in the cross direction. At the same time, the conditions for pore formation are more favorable in the system prepared at the highest λ with better lamellar alignment. Again, the schematic model [Fig. 8(c) and 9(c)] can offer a structural explanation of differences in sound velocities in membranes with different lamellar organization and, consequently, also with a different pore arrangement.

CONCLUSIONS

This study demonstrated the possibility to characterize the structural transformations during the formation of polyethylene porous films and the development of orientation at each stage of structure formation by the combination of X-ray diffraction and sound propagation methods. The values of the sound velocity reflect not only molecular orientation and supermolecular arrangement, but also the occurrence of microscopic pores. The appearance of holes between lamellae is manifested by unexpected results when sound velocity in the orientation direction becomes lower than in the transverse direction where sound waves can propagate through a continuous crystalline phase.

The difference between the sonic modulus calculated from the sound velocity and the Young's modulus obtained from tensile testing can be explained by the heterogeneity of the extruded and annealed films and particularly by the heterogeneity of the porous membranes. The relation between elasticity and sound propagation in such heterogeneous systems is more complex than is predicated by the simple eq. (1). It should be also noted that the wavelength of the sonic signal used brings about some limitations. The test cannot be used as a defectoscopic method that would give the real pore size or its distribution. On the other

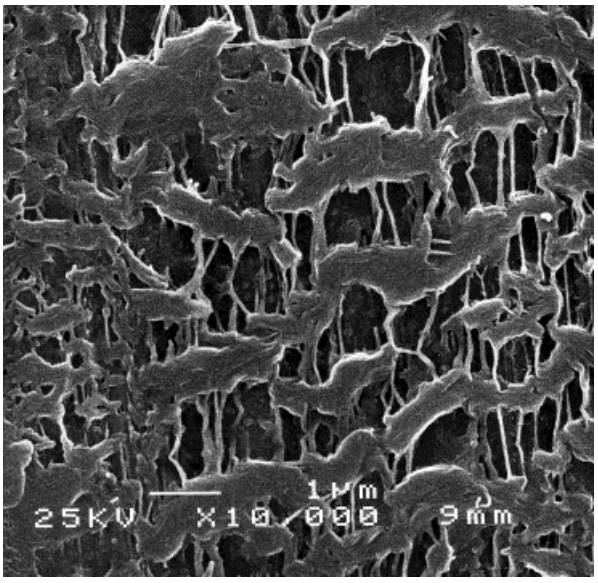

Figure 10 SEM micrograph of a surface of microporous membrane. Bar = 1 μm (courtesy Dr. F. Lednický).

hand, as demonstrated in this study, the polar diagrams of sound propagation give unique structural information that cannot be obtained by other methods.

This work was supported by the Russian Foundation of Fundamental Investigations (Grant No. 98-03-33384a). The financial contributions from the Grant Agency of the Academy of Sciences of the Czech Republic (Grant No. A4050904) and the Grant Agency of the Czech Republic (Grant No. 106/98/0718) are also gratefully acknowledged by the authors. The authors are also indebted to Dr. F. Lednický (IMC Prague) for an SEM micrograph of the microporous membrane.

REFERENCES

1. Sprague, B. S. J Macromol Sci 1973, 8, 157.
2. Park, I. K.; Noether, H. D. Colloid Polym Sci 1975, 53, 824.
3. Karpov, E. A.; Lavrentyev, V. K.; Rosova, E. Yu.; Elyashevich, G. K. Polym Sci A (translated from Russian) 1995, 37, 1247.
4. Peterlin, A. Polym Eng Sci 1976, 16, 126.
5. Frenkel, S. J Polym Sci Polym Symp 1977, 58, 195.
6. Elyashevich, G. K.; Karpov, E. A.; Rosova, E. Yu.; Streltses, B. V.; Marikhin, V. A.; Myasnikova, L. P. Polym Eng Sci 1993, 33, 1341.
7. Kesting R. E. Synthetic Polymer Membranes; Wiley: New York, 1985.
8. Elyashevich, G. K.; Kozlov, A. G.; Rosova, E. Yu. Polym Sci A (translated from Russian) 1998, 40, 956.
9. Elyashevich, G. K.; Kozlov, A. G.; Moneva, I. T.; Zinchik, A. A.; Smirnov, A. V.; Stafeev, S. K. Proc Int Soc Opt Eng (SPIE) 1998, 3573, 296.
10. Raab, M.; Hnát, V.; Kudrna, M. Polym Test 1986, 6, 447.
11. Ziabicki, A. Fundamentals of Fiber Formation; Wiley: New York, 1976.
12. Geil, P. H. Polymer Single Crystals; Interscience: New York, 1962.
13. Rosova, E. Yu.; Karpov, E. A.; Lavrentyev, V. K.; Elyashevich, G. K. In 12th International Annual Meeting of the Polymer Processing Society, Sorrento, Italy, Extended Abstracts, 1996; p 317.
14. Wunderlich, B. Macromolecular Physics; Academic: New York, 1976; Vol. 2.
15. Elyashevich, G. K.; Kozlov, A. G.; Moneva, I. T. Polym Sci B (translated from Russian) 1998, 70, 71.
16. Raab, M.; Ščudla, J.; Kozlov, A. G.; Moneva, I. T.; Elyashevich, G. K. In Book of Abstracts, 18th Discussion Conference "Mechanical Behaviour of Polymeric Materials"; Institute of Macromolecular Chemistry, Prague, Czech Republic, 1998; Abstract PC33.